

Growth of ZnO nanorods on patterned templates for efficient, large-area energy scavengers

G. Niarchos · E. Makarona · C. Tsamis

Received: 16 September 2009 / Accepted: 13 January 2010 / Published online: 12 February 2010
© Springer-Verlag 2010

Abstract ZnO nanostructures were grown on patterned Si substrates using a cost-efficient, low-temperature process, for their future exploitation as functional cores of nanopiezotronic applications. Different substrates and growth parameters were examined in order to determine the optimum process window that will constitute a reliable, low-cost method for large-scale ZnO nanorod production. Statistical analysis was performed to assess the size and shape distribution of the nanorods in an effort to determine the energy conversion efficiency of the resulting structures.

1 Introduction

Over the past few years, ZnO due to its unique set of properties has been the center of attention for a variety of applications. Apart from its use in electronic and optoelectronic devices, such as field-effect transistors (Kwon et al. 2008), gas sensors (Farmakis et al. 2008), solar cells (Law et al. 2005) and UV emitting diodes (Lim et al. 2006), ZnO has showed a great potential for energy-harvesting applications (Wang et al. 2006; Ahmad et al. 2009). Due to its coupled piezoelectric and semiconducting properties, ZnO in the form of nanostructures such as wires, rods or helices (Yong et al. 2008; Wang 2008) has exhibited a remarkable efficiency in the conversion of mechanical energy to electrical energy, becoming thus an excellent candidate for energy scavengers and innovative nanopiezotronic applications.

A number of techniques have been explored so far for the growth of ZnO nanostructures, from vapor–solid–liquid method (VLS) to molecular beam epitaxy (MBE) or metal–organic chemical vapor deposition (MOCVD). However, most of these methods require the use of metal catalysts to promote the growth, resulting in impurity doping of the nanostructures, which can have an impact on the physical properties and the performance of the emerging structures. Moreover, most of these techniques demand growth conditions which are not in accordance with the economic and technological requirements of mass production, since they are mostly suited for laboratory niche applications and proof-of-concept demonstrations. To avoid these limitations, an alternative aqueous chemical growth (ACG) process has been successfully demonstrated as a low-cost, repeatable and reliable method for large-scale production (Vayssieres 2004; Greene et al. 2006; Makarona et al. 2008; Xu et al. 2008).

The core of the ACG process lies in improving the thermodynamics and kinetics of nucleation, growth and ageing of a system through experimentally controlling its interfacial tension (Vayssieres 2004). Growth of the nanostructures begins as metal precursors are being hydrolyzed in a heated aqueous solution of fixed pH and concentration. The whole process is performed in temperatures below 100°C in closed containers, causing it to be environmental-friendly, cost-efficient and most importantly compatible with standard silicon-based microfabrication techniques.

This work focuses on the investigation of the growth parameters of ZnO nanorods on patterned Si substrates using the ACG process. The parameters explored were (a) the concentration of the metal precursor and (b) the effect of different substrates. Based on the results, a statistical analysis was performed examining the nanorods' shapes

G. Niarchos (✉) · E. Makarona · C. Tsamis
Institute of Microelectronics, NCSR “Demokritos”, P. Grigoriou
and Neapoleos St, Aghia Paraskevi, 153 10 Athens, Greece
e-mail: gniarchos@imel.demokritos.gr
URL: <http://www.imel.demokritos.gr>

and sizes. This analysis is a necessary prerequisite for the estimation of the piezoelectric potential distribution and voltage output as a function of the shape and size of the ZnO nanorods when subjected to mechanical deformations (Wang and Song 2006; Niarchos et al. 2009b).

2 Experimental

This study explored the effect of three different substrates: (a) bare Si(100) wafers, used as reference, (b) Si(100) wafers covered with a 50-nm thick Au film (over an intermediate 20-nm thick Ti adhesion layer), and (c) Si(100) wafers covered with a uniform 150-nm thick ZnO seeding layer. Both the Au and ZnO seeding layers were deposited by RF magnetron sputtering. The Au covered wafers were subjected to a 1-h long post-deposition annealing in vacuum at 300°C. Earlier experimental results (Niarchos et al. 2009a) have shown that as-sputtered ZnO seeding films do not require further post-deposition treatment for the successful growth, therefore substrates (c) were used as obtained. After sputtered all substrates were cleaned in ultrasonic baths of acetone, propanol and deionized water for 10 min prior to the ZnO-growth step.

During the ACG growth the samples were placed face down in aqueous solutions containing equimolar amounts of zinc nitrate hexahydrate $[\text{Zn}(\text{NO}_3)_2 \cdot 6\text{H}_2\text{O}]$ and hexamethylenetetramine (HMTA) ranging from 5 to 100 mM. During the hydrothermal process, divalent zinc solvated in water produces Zn^{+2} aquo ions (Vayssieres 2004), which as most divalent metal ions, have a low tendency of precipitation by hydrolysis–condensation in neutral or acidic solutions. For that reason HMTA is introduced into the aqueous solution to increase the pH and thus promote the ZnO precipitation; however, the exact role HMTA plays is still under debate. Based on the theoretical model

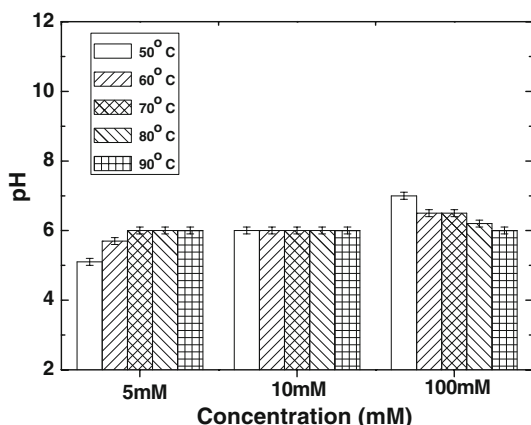


Fig. 1 pH dependence on the concentration of zinc acetate/HMTA and the temperature

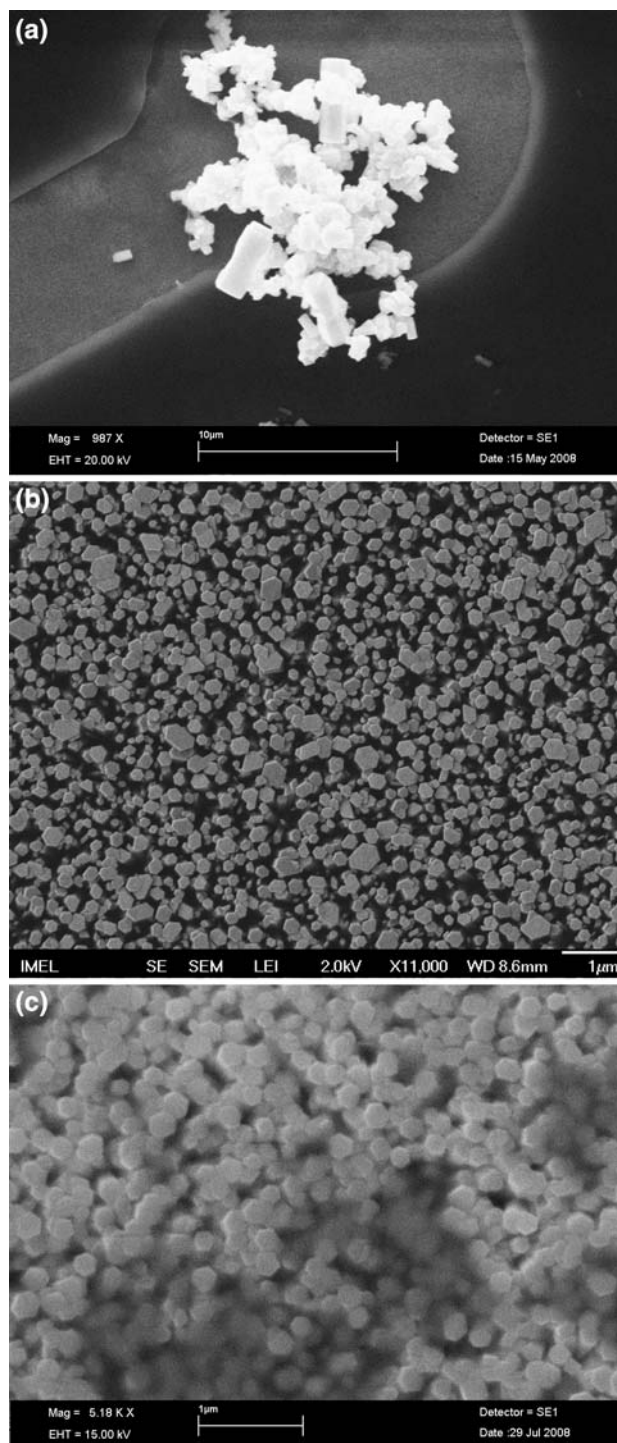


Fig. 2 SEM images of ZnO nanostructures after a 4 h ACG on Si substrates with ZnO seeding layer **a** $T = 50^\circ\text{C}$, $\text{pH} 5$, $C = 5 \text{ mM}$, **b** $T = 90^\circ\text{C}$, $\text{pH} 6$, $C = 10 \text{ mM}$, and **c** $T = 90^\circ\text{C}$, $\text{pH} 6$, $C = 100 \text{ mM}$

(Vayssieres 2004), controlling the pH changes the surface charge density at the nucleation sites, which, in turn, affects the size and shape of the produced nanostructures. However, the size and shape of the nanostructures are also greatly affected by the temperature. From our results

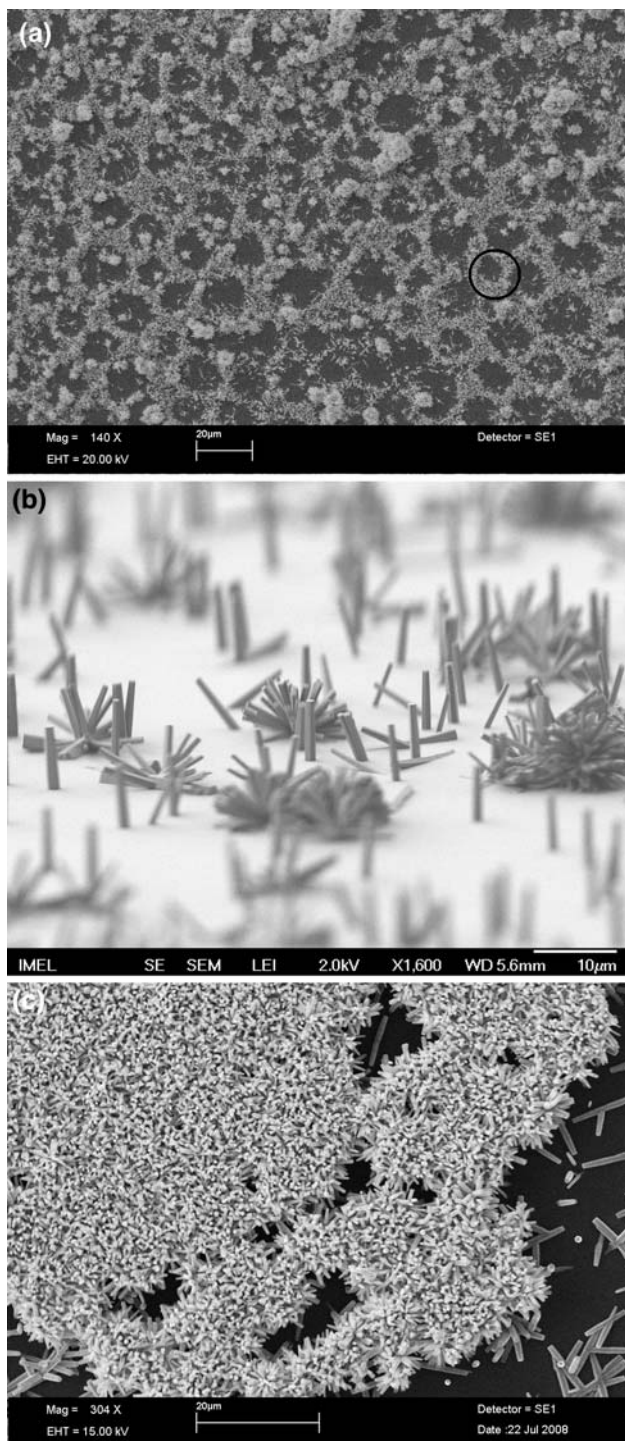


Fig. 3 SEM images of ZnO nanostructures grown on Si substrates with Au seeding layer ($T = 90^{\circ}\text{C}$, $C = 10\text{ mM}$), **a** spontaneous organization on honeycomb “lattices”, **b** magnification of the encircled area of **a** where coexistence of multi-angular and vertical nanorods is shown and **c** ZnO nanostructures grown under the same conditions on a bare Si reference sample

(Niarchos et al. 2009a) and in accordance with the theory of nucleation (Vayssieres 2004) and other reports (Xu et al. 2008; Cui et al. 2005), low-aspect ratio nanorods of mixed

zinc-blende and wurtzite structures are produced at lower temperatures ($50\text{--}70^{\circ}\text{C}$), while slightly higher temperatures ($80\text{--}90^{\circ}\text{C}$) promote wurtzite-dominant, high-aspect ratio nanorods. Matters are further complicated since the temperature affects—apart from the reaction kinetics—the pH of the solution. The effect of HMTA concentration and temperature in controlling the pH and the reaction dynamics and kinetics is illustrated in Fig. 1. Acidic ($\text{pH} \sim 5$) or basic ($\text{pH} \sim 7$) solutions regardless of the reactant concentration resulted into scant low-aspect ratio zinc-blende-dominated structures (Fig. 2a). In contrast, keeping the pH slightly acidic ($\text{pH} \sim 6$) resulted into substrates covered with high-aspect ratio wurtzite nanorods with high surface coverage (Fig. 2b, c). In addition, it can be seen that only at 90°C the pH can accurately be controlled for any concentration range (Fig. 1). Since the ultimate goal is to find a cost-efficient and facile method to grow vertically aligned ZnO nanostructures for energy-harvesting applications, the temperature was opted to be kept at 90°C (i.e. the pH kept constant at 6) for all experiments so as to elucidate the role of the other growth parameters.

3 Results and discussion

Even though the ACG process offers the flexibility of growth in any flat surface, the morphology and orientation of the resulting nanostructures is quite hard to control, due to the interlaced dependence on all growth parameters (pH, concentration, time, temperature and substrate). In Si(100) substrates this was observed quite clearly, as the ZnO nanostructures were not only non-uniformly grown across the wafer’s surface but also tended to sprout from nucleation sites in a multi-angular way (inset Fig. 3a). In spite the fact that for all concentrations used, the length and

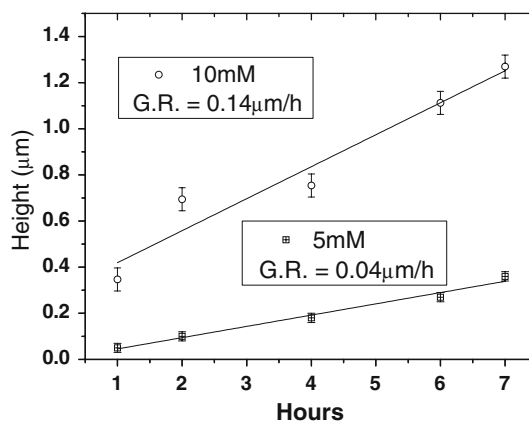


Fig. 4 Growth rate of ZnO nanorods at 5 and 10 mM ($T = 90^{\circ}\text{C}$, pH 6)

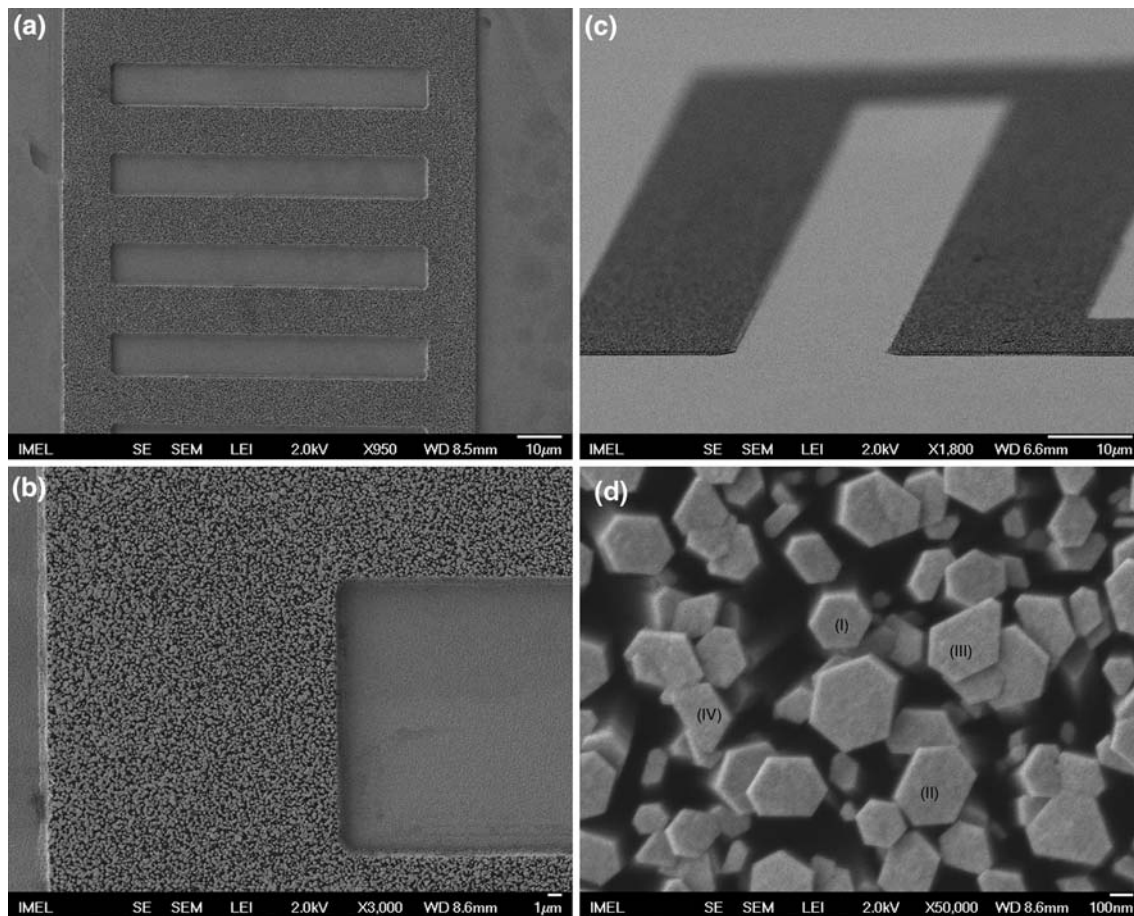


Fig. 5 SEM images of ZnO nanorods of high cover density and uniformity grown on Si substrates with ZnO seeding layer after 7 h of ACG at $T = 90^{\circ}\text{C}$ with nutrient concentration of **a, b** 10 mM and **c**

5 mM, **(d)** magnification where the various types of resulting rods are shown: *(I)* regular, *(II)* elongated, *(III)* asymmetric, and *(IV)* non-hexagonal rods

cover density increased with time, these nanostructures cannot serve an application that requires uniform coverage with vertical orientation.

For the Si substrates covered with Au the annealing of the Au surface led to the promotion of ZnO structures grown spontaneously on hexagonal (honeycomb) “lattices”. In high concentrations (>10 mM), hexagonal patterns were clearly observed (Fig. 3a), whereas for low concentrations (<10 mM) the patterns were not visible even after 7 h of continuous growth (Niarchos et al. 2009a). Despite the self-assembly of the structures, vertically aligned nanorods co-existed with “flower”-like shapes with the vertically aligned rods being an order of magnitude larger both in height and in width (Fig. 3b). In addition, the “flower”-like structures had only grown along the lines of the hexagonal lattices, whereas the vertical rods (Fig. 3b) had the tendency to sprout isolated within the centers of the hexagons. In the case of the most dilute solutions, no organization was to be found in the growth of the nanostructures, while both the “flower”-like and the isolated vertical rods had similar dimensions (Niarchos

et al. 2009a). Since the pH was the same for all concentration ranges, it seems that the concentration of the reactants is the key factor in controlling the size of the grown nanostructures. As a general trend, dilute solutions (≤ 10 mM) result in thinner rods that lack organization, while denser solutions provide thicker nanostructures that have a spontaneous organization into honeycomb “lattices”. Still, Au films as the seeding layer does not provide any control over the orientation of the nanorods while is a critical parameter for the development of nanopiezoelectric applications.

As a last approach, Si(100) wafers covered with a thin (<300 nm) ZnO seeding layer were used. The as-sputtered ZnO film successfully promoted the growth of highly uniform, densely packed vertically aligned nanorods for the entire concentration range examined (5–100 mM). By decreasing the concentrations of the reactants, the mean diameter of the nanorods decreased from ~ 350 to ~ 100 nm, but a reduction in length was also observed from 1.3 to ~ 400 nm, in accordance with Vayssieres (2004). At high concentrations (>50 mM), coalescence of

the nanorods, that tended to fuse into a film, was observed after 7 h of growth. Lower concentrations (<10 mM) provided a means of more accurate control over the dimensions of the nanostructures as a function of the growth time (Niarchos et al. 2009a) (Fig. 4).

Since accurate control of the dimensions and sizes of the resulting nanostructures was achieved by employing the ZnO seeding layer, lithographically patterned substrates were the next step towards exhibiting the potential of the ACG to become a low-cost, environmental-friendly method for large-scale mass production. Si(100) wafers with 150-nm thick ZnO seeding layers were patterned with standard optical lithography (the size of the patterns ranging from 5 to 80 μm). The samples were placed face down for 7 h onto the surface of the nutrient solutions of low reactant concentrations (5–10 mM) at a fixed temperature of 90°C and pH 6. After the ACG step the samples were rinsed in DI water and dried in air. A standard lift-off procedure and rinsing in organic solvents for the removal of residual photoresist followed. Vertically aligned nanorods were grown with high cover density and uniformity (Fig. 5a, b) onto the various patterns where the vertical alignment seemed to be further enhanced by the physical confinement of the photoresist side-walls. It is worth noting that the growth follows even the lithographic imperfections and the undercuts of the photoresist (Fig. 5c).

The ACG process has proven quite efficient in successfully growing vertically aligned ZnO nanorods on patterned substrates. Such features can be used in energy-harvesting applications as a means to convert mechanical energy to electrical energy. However, in order to design an efficient mechanical scavenger, theoretical analysis is required that will take into account, not only the estimated potential distribution of a single nanorod when subjected to a mechanical deformation, but also the actual shape and size distribution of the nanorod as a function of the processing technology (Niarchos et al. 2009b). Thus, detailed statistical analysis of these characteristics is required in order to be able to predict the electrical characteristics of a dense array of ZnO nanorods. Statistical analysis was performed on $20 \times 20 \mu\text{m}^2$ SEM images and over 700 nanorods were measured per condition.

The various shapes of the resulting nanostructures grown by the process described and identified in this work can be seen in Fig. 5d and are classified into four different types: (I) regular hexagonal-shaped, (II) elongated hexagonal-shaped, (III) asymmetric hexagonal-shaped, and (IV) Irregular (non-hexagonal) shaped nanorods. Figure 6a shows the distribution of the hexagonal-shaped (Types I, II, and III) and non-hexagonal (type IV) ZnO nanorods over the patterned areas. It can be seen that the number of hexagonal-shaped nanorods is significantly larger (80–85%) compared to the irregularly shaped ones, indicating

that the process conditions favour the growth of hexagonal based structures. From the same figure, it can be seen that the ratio of hexagonal to non-hexagonal structures is within experimental error, independent of the concentration of the aqueous solution. However, the decrease of the reactant concentration from 10 to 5 mM (even in the dilute solution) decreased significantly the percentage of regular hexagonal nanorods (Type I), while the number of elongated (Type II) and asymmetric (Type III) nanorods increased, respectively. This fact further underlined the importance of the reactant concentration and its prominent role in the growth.

Another key issue one needs to examine is the size distribution of the nanorods. The diameter distribution of the hexagonal-shaped nanorods of types I, II, and III is shown in

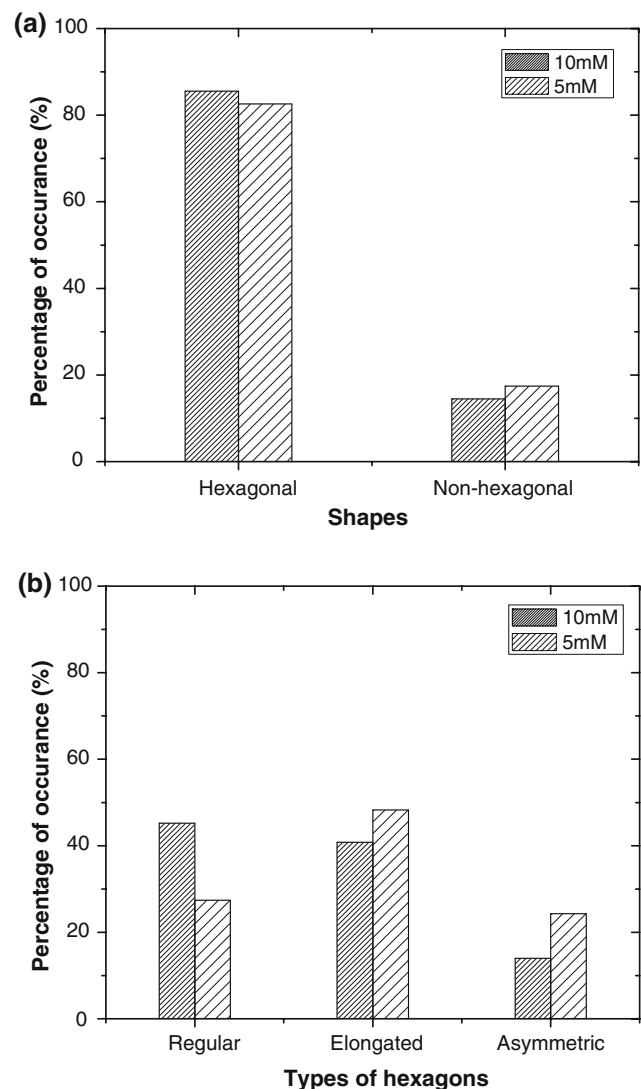


Fig. 6 a Distribution of hexagonal and non-hexagonal structures on wafer, b distribution of various types of hexagons grown at various solution concentrations

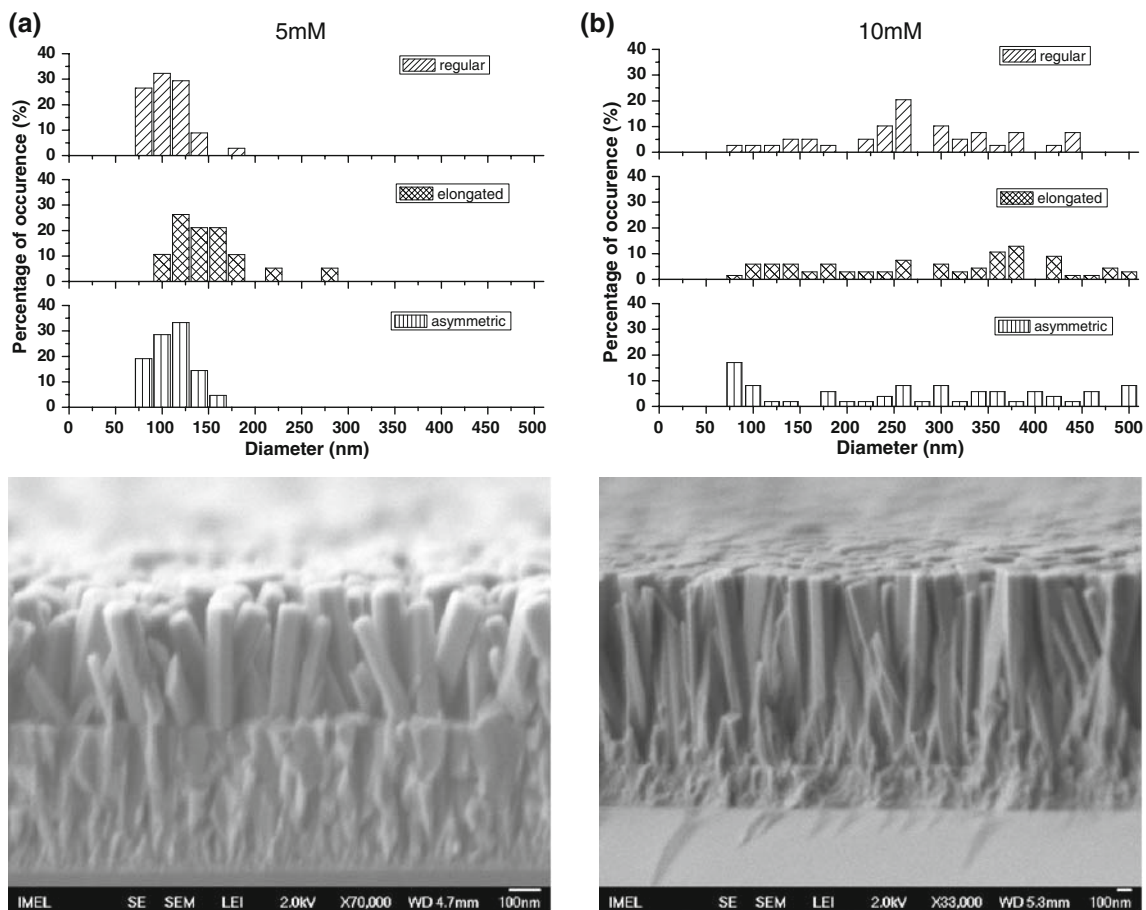


Fig. 7 Diameter dispersion of the various hexagonal nanorods grown in **a** 5 mM and **b** 10 mM solutions for 7 h at $T = 90^{\circ}\text{C}$. *Bottom insets:* cross-sections of the patterned substrates

Fig. 7. It can be seen that slightly increased concentrations (10 mM) allow for the production of more uniform and denser arrays but with a compromise on the precision of the size control. On the other hand, however, the lowest concentration, nutrient solutions (5 mM) provide a better control over the size dispersion of the produced nanorods.

4 Conclusions

A facile and cost-efficient method for the controllable growth of uniform vertically oriented ZnO nanorods over large areas has been determined. The method consists of a hydrothermal growth step during which the key factors determining the size of the resulting structures is the accurate control of the pH through the interplay of temperature and the reactants concentration. The method is fully compatible with conventional microfabrication techniques and can be used for the production of dense and uniform ZnO nanorods on patterned templates of any size on the wafer scale. A statistical analysis of the size and

shape distribution of the nanorods was performed and it was established that there is a compromise between size/growth rate and size uniformity. Depending on the targeted application the proposed method can procure patterns containing either highly uniform nanorods of smaller-aspect ratio or of high-aspect ratio rods of moderate size dispersion. Finally, the statistical analysis can form the basis of more extensive simulations determining the energy conversion efficiency of the patterned templates as a function of the nanostructures shapes and sizes.

Acknowledgments The research is funded by National Funds and the European Regional Development Fund in the framework of NSRF 2007–2013, contract no. 45. The authors would like to thank Dr. Th. Speliotis for preparation of ZnO films and E. Linarakis for assistance with the SEM measurements.

References

- Ahmad U, Al-Hajry A, Hahn YB, Kim DH (2009) Rapid synthesis and dye-sensitized solar cell applications of hexagonal-shaped ZnO nanorods. *Electrochim Acta* 54:5358–5362

- Cui JB, Daghljan CP, Gibson UJ, Pusche R, Geithner P, Ley L (2005) Low-temperature growth and field emission of ZnO nanowire arrays. *J Appl Phys* 97:044315
- Farmakis FV, Speliotis Th, Alexandrou KP, Tsamis C, Kompitsas C, Fasaki I, Jedrasik P, Petersson G, Nilsson B (2008) Field-effect transistors with thin ZnO as active layer for gas sensor applications. *Microelectron Eng* 85:1035–1038
- Greene LE, Yuhas BD, Law M, Zitoun D, Yang P (2006) Solution-grown zinc oxide nanowires. *Inorg Chem* 45(19):7535–7543
- Kwon SS, Hong WK, Jo G, Maeng J, Kim TW, Song S, Lee T (2008) Piezoelectric effect on the electronic transport characteristics of ZnO nanowire field-effect transistors on bent flexible substrates. *Adv Mater* 20(23):4557–4562
- Law M, Greene LE, Johnson JC, Saykally R, Yang P (2005) Nanowire dye-sensitized solar cells. *Nat Mat* 4:455–459
- Lim JH, Kang CK, Kim KK, Park IK, Hwang DK, Park SJ (2006) UV electroluminescence emission from ZnO light-emitting diodes grown by high-temperature radiofrequency sputtering. *Adv Mater* 18(20):2720–2724
- Makarona E, Speliotis T, Niarchos G, Niarchos D, Tsamis C (2008) ZnO nanorod growth based on a low-temperature silicon-compatible combinatorial method. *Phys Stat Sol C* 5(12):3809–3812
- Niarchos G, Makarona E, Tsamis C (2009a) Growth of ZnO nanorods on patterned templates for energy harvesting applications. *Proc SPIE* 7362:73621L-1
- Niarchos G, Makarona E, Tsamis C (2009b) Modeling and optimization of ZnO nanostructure arrays for improved energy conversion efficiency. Presented at the 3rd international conference on one-dimensional nanomaterials (ICON) on December 7–9. Georgia Institute of Technology, Atlanta
- Vayssieres L (2004) On the design of advanced metal oxide nanomaterials. *Int J Nanotechnol* 1(1/2):1–41
- Wang ZL (2008) Towards self-powered nanosystems: from nanogenerators to nanopiezotronics. *Adv Funct Mater* 18:1–15
- Wang ZL, Song JH (2006) Piezoelectric nanogenerators based on zinc oxide nanowire arrays. *Science* 312:242–246
- Wang X, Zhou J, Song J, Liu J, Ningsheng X, Wang ZL (2006) Piezoelectric field effect transistor and nanoforce sensor based on a single ZnO nanowire. *Nano Lett* 6(12):2768–2772
- Xu S, Lao G, Weintraub B, Wang ZL (2008) Density controlled growth of aligned ZnO nanowire arrays by seedless chemical approach on smooth surfaces. *J Mater Res* 23(8):2072–2077
- Yong Q, Xudong W, Zhong Lin W (2008) Microfibre–nanowire hybrid structure for energy scavenging. *Nature* 451:809–813